Oral presentation | Numerical methods

Numerical methods-IV

Wed. Jul 17, 2024 2:00 PM - 4:00 PM Room A

[8-A-02] Application of Hybrid MUSCL-THINC Approach to Magnetohydrodynamic Simulations for Sharply Capturing Discontinuities

*Tomohiro Mamashita[1], Gaku Fukushima[1], Keiichi Kitamura[1] （1. Yokohama National University）

Keywords: magnetohydrodynamics (MHD), reconstruction scheme, MUSCL, THINC

The 12th International Conference on Computational Fluid Dynamics

8-A-02

Application of Hybrid MUSCL-THINC Approach to Magnetohydrodynamic Simulations for Sharply Capturing Discontinuities

○ Tomohiro Mamashita (Yokohama National University)
Gaku Fukushima† (Yokohama National University)
Keiichi Kitamura (Yokohama National University)

† Currently affiliated with Université de Sherbrooke

Outline

[1] https://sdo.gsfc.nasa.gov/assets/img/browse/2010/08/19/20100819_003221_4096_0304.jpg
[2] Yoshino, T., Fujino, T. and Ishikawa, M., "Possibility of Thermal Protection in Earth Re-entry Flight by MHD Flow Control with Air-Core Circular Magnet," *IEEJ Trans Elec Electron Eng*, **4**(2009), 510-517.
[3] https://soken.nifs.ac.jp/en/archives/about/simulation_course

Background & Objective

■ Application of magnetohydrodynamics

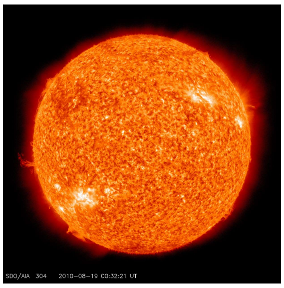

Solar internal current [1]

Astrophysics

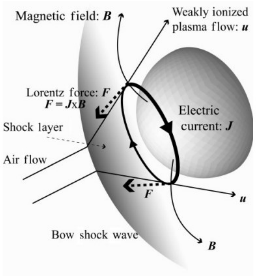

Thermal protection system for re-entry capsule
MHD flow control [2]

Aerospace Engineering

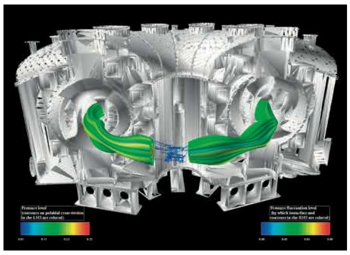

MHD simulation of LHD
(Large Helical Device) plasma [3]

Nuclear fusion

Magnetohydrodynamics (MHD) can deal with macroscopic phenomena caused by the interaction of plasma flow and magnetic fields and is applied in many research fields.

Computational fluid dynamics (CFD) is often used as an effective research tool.

Background & Objective

■ Finite volume method

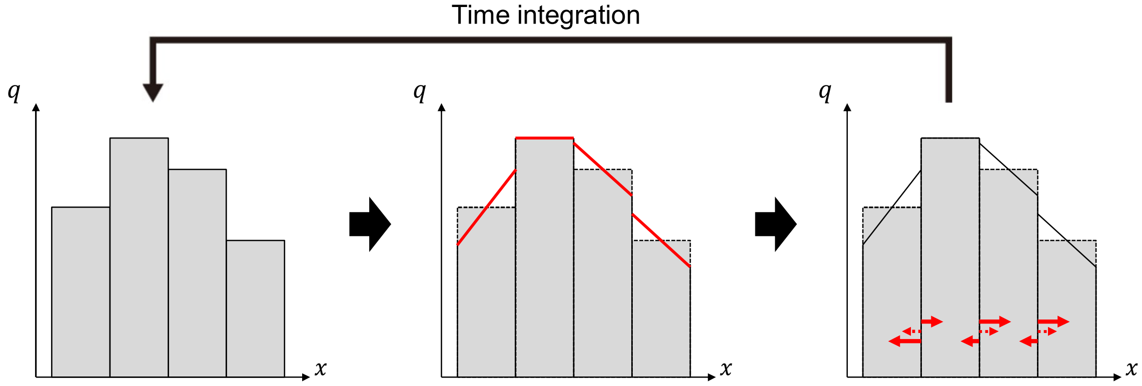

Initial data

Reconstruction

Flux calculation

Data reconstruction prior to the flux calculation can improve the accuracy of the calculation.

The slope is limited for numerical stabilization near discontinuities such as shock waves.

Background & Objective

■ Reconstruction schemes

MUSCL [4]

Advantage:
- Robust
- Low calculation cost
- Easy to apply to unstructured grid systems

Drawback:
- Dissipative

Higher order schemes (WENO [5]**, MP** [6] **and others)**

Advantage:
- High resolution

Drawback:
- High calculation cost
- Difficult to apply to unstructured grid systems (owing to large stencil size)

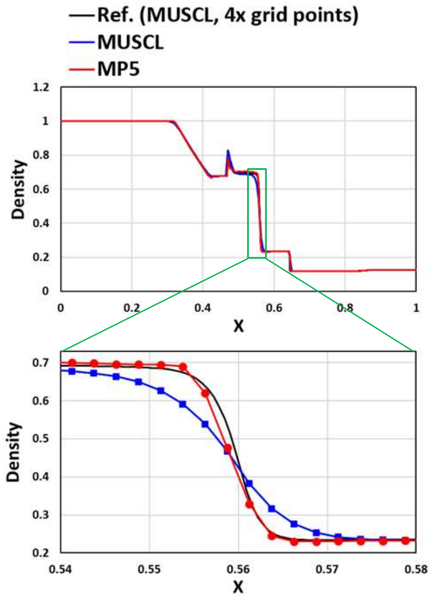

MHD shock tube test

[4] Van Leer, B., "Towards the ultimate conservative difference scheme V. A second order sequel to Godunov's method," J. Comput. Phys. 32 (1979) 101–136.
[5] Liu, X. D., Osher, S., and Chan, T., "Weighted essentially non-oscillatory schemes," J. Comput. Phys. 115 (1994) 200–212.
[6] Suresha, A. and Huynh, H. T., "Accurate monotonicity-preserving schemes with Runge-Kutta time stepping," J. Comput. Phys. 136 (1997) 83–99.

Background & Objective

■ Hybrid MUSCL-THINC (MT) [7]

$$\boxed{V^{\mathrm{MT}} = (1-\zeta)V^{\mathrm{MUSCL}} + \zeta V^{\mathrm{THINC}}}$$

● MUSCL

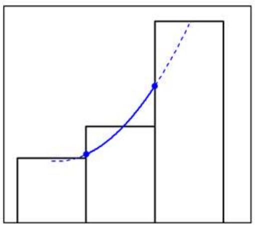

Use polynomial function

$$\hat{V}_i^{\mathrm{MUSCL}}(x) = V_i + \frac{V_{i+1}-V_{i-1}}{2\Delta x}(x-x_i) + \frac{3\kappa}{2}\frac{V_{i+1}-2V_i+V_{i-1}}{\Delta x^2}\left[(x-x_i)^2 - \frac{\Delta x^2}{12}\right]$$

→ For resolving smooth regions

● THINC

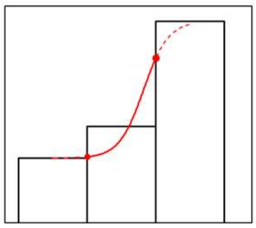

Use hyperbolic tangent function

$$\hat{V}_i^{\mathrm{THINC}}(x) = \min(V_{i-1}, V_{i+1}) + \frac{|V_{i+1}-V_{i-1}|}{2}\{1+\theta\tanh[\beta(X_i-d_i)]\}$$

→ For resolving discontinuous distributions

[7] Chiu, T. Y., Niu, Y. Y., and Chou, Y. J., "Accurate Hybrid AUSMD Type Flux Algorithm with Generalized Discontinuity Sharpening Reconstruction for Two-Fluid Modeling," J. Comput. Phys., 443 (2021), 110540.

Background & Objective

■ Hybrid MUSCL-THINC (MT) [7]

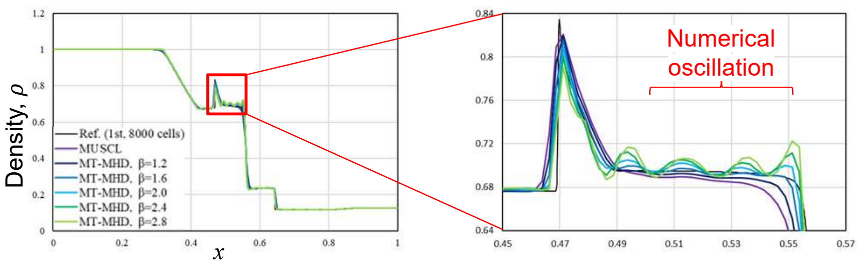

Overall view

Vicinity of compound wave

MHD shock tube test

From our preliminary numerical experiments, applying MT to MHD simulations results in oscillatory solutions.

Objective:

- Apply MT to MHD simulations.
- Present a method where complex MHD discontinuities are captured robustly and sharply.

[7] Chiu, T. Y., Niu, Y. Y., and Chou, Y. J., "Accurate Hybrid AUSMD Type Flux Algorithm with Generalized Discontinuity Sharpening Reconstruction for Two-Fluid Modeling," J. Comput. Phys., 443 (2021), 110540.

Outline

Governing Equations

■ Ideal MHD equation (conservation form)

MHD has governing equations that incorporate **Faraday's law of induction** into the fluid equations.

● Gas dynamics

$$\frac{\partial \boldsymbol{U}}{\partial t} + \nabla \cdot \boldsymbol{F} = 0$$

$$\boldsymbol{U} = \begin{pmatrix} \rho \\ \rho \boldsymbol{v} \\ e \end{pmatrix}, \boldsymbol{F} = \begin{pmatrix} \rho \boldsymbol{v} \\ \rho \boldsymbol{v}\boldsymbol{v} + p\boldsymbol{I} \\ (e+p)\boldsymbol{v} \end{pmatrix}$$

● MHD

$$\frac{\partial \boldsymbol{U}}{\partial t} + \nabla \cdot \boldsymbol{F} = 0$$

$$\boldsymbol{U} = \begin{pmatrix} \rho \\ \rho \boldsymbol{v} \\ e \\ \boldsymbol{B} \end{pmatrix}, \boldsymbol{F} = \begin{pmatrix} \rho \boldsymbol{v} \\ \rho \boldsymbol{v}\boldsymbol{v} + p_T\boldsymbol{I} - \boldsymbol{B}\boldsymbol{B} \\ (e+p_T)\boldsymbol{v} - \boldsymbol{B}(\boldsymbol{v}\cdot\boldsymbol{B}) \\ \boldsymbol{v}\boldsymbol{B} - \boldsymbol{B}\boldsymbol{v} \end{pmatrix}$$

Induction equation

Governing Equations

■ Characteristic waves of the gas dynamics and MHD

● Gas dynamics

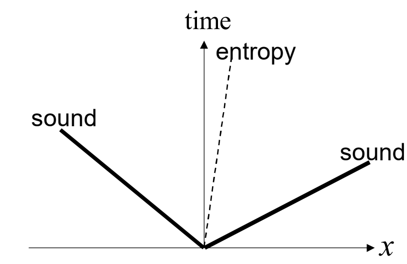

→ 3 waves

- Shock wave
- Tangential discontinuity
- Contact discontinuity

● MHD

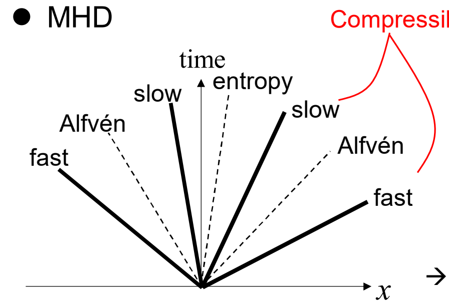

→ 7 waves

- Fast shock wave
- Slow shock wave
- Tangential discontinuity
- Contact discontinuity
- Rotational discontinuity

The MHD Riemann problem has more characteristic waves. → There is a variety of MHD discontinuities.

Outline

Methodology

■ MUSCL [4]

Interpolation function using a quadratic polynomial:

$$\hat{V}_i^{\mathrm{MUSCL}}(x) = V_i + \frac{V_{i+1} - V_{i-1}}{2\Delta x}(x - x_i) + \frac{3\kappa}{2}\frac{V_{i+1} - 2V_i + V_{i-1}}{\Delta x^2}\left[(x - x_i)^2 - \frac{\Delta x^2}{12}\right]$$

Cell interface values with a slope limiter:

$$\begin{cases} \hat{V}_{L,i+1/2}^{\mathrm{MUSCL}} = V_i + \dfrac{1-\kappa}{4}\psi(r)(V_i - V_{i-1}) + \dfrac{1+\kappa}{4}\psi\left(\dfrac{1}{r}\right)(V_{i+1} - V_i), \\ \hat{V}_{R,i-1/2}^{\mathrm{MUSCL}} = V_i - \dfrac{1-\kappa}{4}\psi\left(\dfrac{1}{r}\right)(V_{i+1} - V_i) - \dfrac{1+\kappa}{4}\psi(r)(V_i - V_{i-1}), \end{cases}$$

The minmod limiter:

$$\psi(r) = \max[0, \min(1, r)].$$

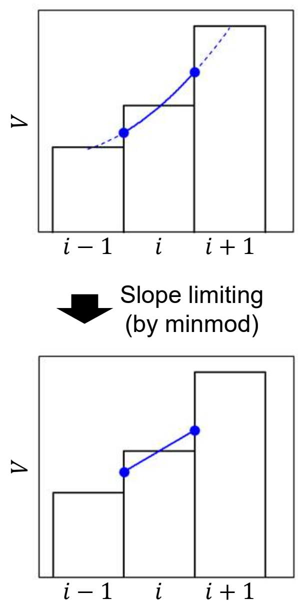

[4] Van Leer, B., “Towards the ultimate conservative difference scheme V. A second order sequel to Godunov’s method,” J. Comput. Phys. 32 (1979) 101–136.

Methodology

■ THINC [8]

Interpolation function using a hyperbolic tangent:

$$\hat{V}_i^{\mathrm{THINC}}(x) = \min(V_{i-1}, V_{i+1}) + \frac{|V_{i+1} - V_{i-1}|}{2}\{1 + \theta \tanh[\beta(X_i - d_i)]\}$$

$$\left(\begin{array}{lll} X_i = \dfrac{x - x_{i-1/2}}{x_{i+1/2} - x_{i-1/2}}, & \theta = \mathrm{sign}(V_{i+1} - V_{i-1}), & d_i = \dfrac{1}{2\beta}\ln\dfrac{1-A}{1+A} \\ A = \dfrac{B/\cosh(\beta) - 1}{\tanh(\beta)}, & B = \exp\left\{\theta\beta\left[\dfrac{2\left(V_i - \min(V_{i-1}, V_{i+1})\right)}{|V_{i+1} - V_{i-1}|} - 1\right]\right\} & \end{array}\right)$$

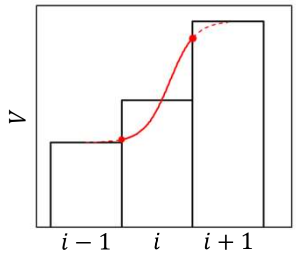

For a monotone distribution

Cell interface values:

$$\begin{cases} \hat{V}_{L,i+1/2}^{\mathrm{THINC}} = V_{\min} + \dfrac{\Delta V}{2}\left\{1 + \theta\dfrac{\tanh(\beta) + A}{1 + A\tanh(\beta)}\right\}, \\ \hat{V}_{R,i-1/2}^{\mathrm{THINC}} = V_{\min} + \dfrac{\Delta V}{2}(1 + \theta A). \end{cases}$$

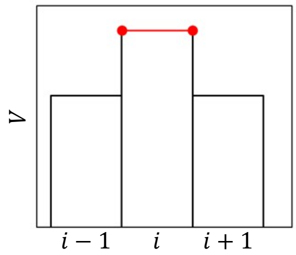

For a local extremum

NOTE: When a target cell is located at a local extremum, the cell is not reconstructed (namely, 1st-order accuracy) because the hyperbolic tangent function cannot be defined.

[8] F. Xiao, Y. Honma, T. Kono,"A simple algebra interface capturing scheme using hyperbolic tangent function ", Int. J. Numer. Methods Fluids, 48, (2005), pp. 1023–1040.

Methodology

■ THINC [8]

Interpolation function using a hyperbolic tangent:

$$\hat{V}_i^{\mathrm{THINC}}(x) = \min(V_{i-1}, V_{i+1}) + \frac{|V_{i+1} - V_{i-1}|}{2}\{1 + \theta \tanh[\beta(X_i - d_i)]\}$$

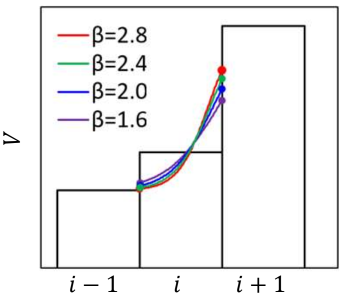

- β is a user-specified parameter.
- β determines a maximum slope of the hyperbolic tangent function.
- A value between $\beta = 1.6 - 3.0$ is generally employed.
- A larger β provides a sharper slope, albeit with the higher risk of numerical oscillations.

[8] F. Xiao, Y. Honma, T. Kono,"A simple algebra interface capturing scheme using hyperbolic tangent function ", Int. J. Numer. Methods Fluids, 48, (2005), pp. 1023–1040.

Methodology

■ Hybrid MUSCL-THINC (MT) [7]

$$\begin{cases} \hat{V}^{\mathrm{MT}}_{L,i+1/2} = (1-\zeta)\hat{V}^{\mathrm{MUSCL}}_{L,i+1/2} + \zeta\hat{V}^{\mathrm{THINC}}_{L,i+1/2} \\ \hat{V}^{\mathrm{MT}}_{R,i-1/2} = (1-\zeta)\hat{V}^{\mathrm{MUSCL}}_{R,i-1/2} + \zeta\hat{V}^{\mathrm{THINC}}_{R,i-1/2} \end{cases}$$

$$\zeta = 1 - \min\left(\frac{\hat{V}^{\mathrm{MUSCL}}_{L,i+1/2} - \hat{V}^{\mathrm{MUSCL}}_{R,i-1/2} + \varepsilon_z}{V_{i+1} - V_i + \varepsilon_z}, \frac{\hat{V}^{\mathrm{MUSCL}}_{L,i+1/2} - \hat{V}^{\mathrm{MUSCL}}_{R,i-1/2} + \varepsilon_z}{V_i - V_{i-1} + \varepsilon_z}\right)$$

$$\zeta \to \begin{cases} 0 & \text{for continuous distributions} & \to \text{MUSCL is dominant.} \\ 1 & \text{for discontinuous distributions} & \to \text{THINC is dominant.} \end{cases}$$

We implemented MT to MHD simulations so that each component of the primitive variable vector $\boldsymbol{V} = (\rho, u, v, w, p, B_x, B_y, B_z)^T$ is reconstructed independently.
This scheme will be called **MT-MHD** in this study.

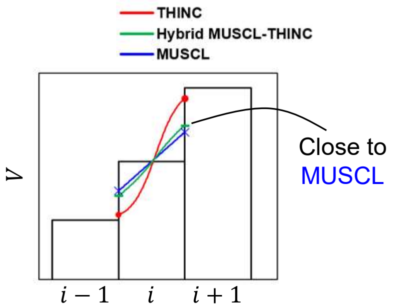

$\zeta \to 0$ for a continuous distribution

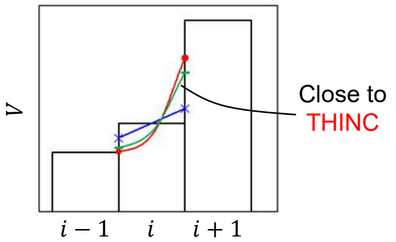

$\zeta \to 1$ for a discontinuous distribution

[7] Chiu, T. Y., Niu, Y. Y., and Chou, Y. J., "Accurate Hybrid AUSMD Type Flux Algorithm with Generalized Discontinuity Sharpening Reconstruction for Two-Fluid Modeling," J. Comput. Phys., 443 (2021), 110540.

Outline

Numerical example

■ Shock tube test of gas dynamics [9]

$$\begin{pmatrix} \rho \\ p \\ u \\ v \\ w \\ B_x \\ B_y \\ B_z \end{pmatrix}_L = \begin{pmatrix} 1 \\ 1 \\ 0 \\ 0 \\ 0 \\ 0 \\ 0 \\ 0 \end{pmatrix} \text{ for } 0 \le x < 0.5, \quad \begin{pmatrix} \rho \\ p \\ u \\ v \\ w \\ B_x \\ B_y \\ B_z \end{pmatrix}_R = \begin{pmatrix} 0.125 \\ 0.1 \\ 0.0 \\ 0.0 \\ 0.0 \\ 0 \\ 0 \\ 0 \end{pmatrix} \text{ otherwise.}$$

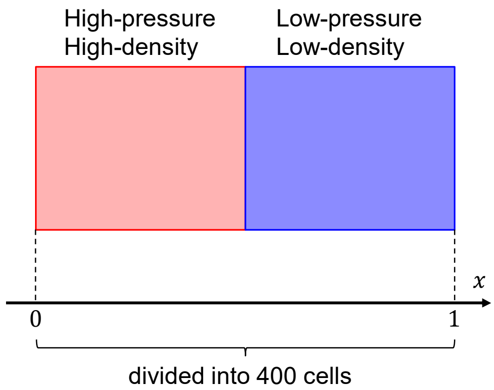

- The computational domain [0, 1] is divided into 400 uniform cells.
- The specific heat ratio is set to $\gamma = 1.4$.

[9] Sod, G. A., "A Survey of Several Finite Difference Methods for Systems of Nonlinear Hyperbolic Conservation Laws", Journal of Computational Physics, vol. 27, No. 1, 1978, pp.1–31.

Numerical example

■ Shock tube test of gas dynamics [9]

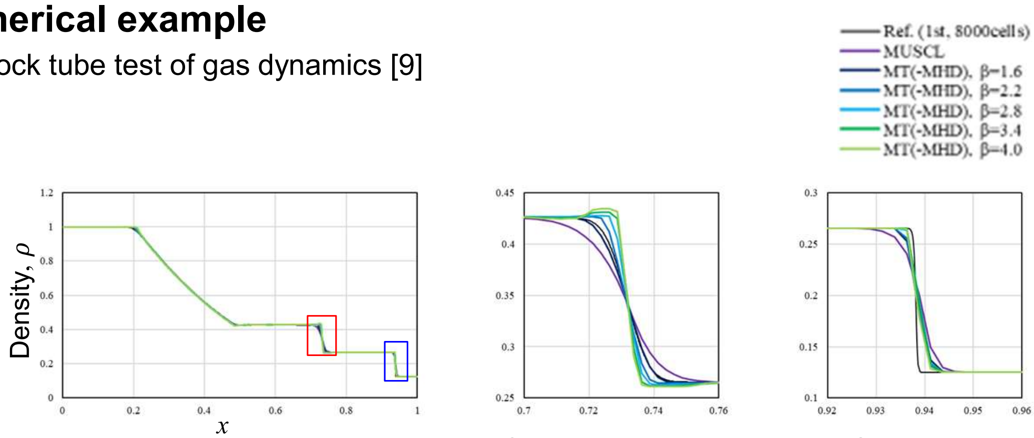

Contact discontinuity

Shock wave

- In this test, MT-MHD is equivalent to MT.
- The discontinuities are sharpened without overshoot if $\beta \le 2.8$.

[9] Sod, G. A., "A Survey of Several Finite Difference Methods for Systems of Nonlinear Hyperbolic Conservation Laws", Journal of Computational Physics, vol. 27, No. 1, 1978, pp.1–31.

[6] Brio, M., and Wu, C.C., “An upwind differencing scheme for the equations of ideal magnetohydrodynamics”, Journal of Computational Physics, vol. 75, 1988, pp.400-422.

Numerical example

■ MHD shock tube test [10]

$$\begin{pmatrix} \rho \\ p \\ u \\ v \\ w \\ B_x \\ B_y \\ B_z \end{pmatrix}_L = \begin{pmatrix} 1.0 \\ 1.0 \\ 0.0 \\ 0.0 \\ 0.0 \\ 0.75 \\ 1.0 \\ 0.0 \end{pmatrix} \text{ for } 0 \leq x < 0.5, \quad \begin{pmatrix} \rho \\ p \\ u \\ v \\ w \\ B_x \\ B_y \\ B_z \end{pmatrix}_R = \begin{pmatrix} 0.125 \\ 0.1 \\ 0.0 \\ 0.0 \\ 0.0 \\ 0.75 \\ -1.0 \\ 0.0 \end{pmatrix} \text{ otherwise.}$$

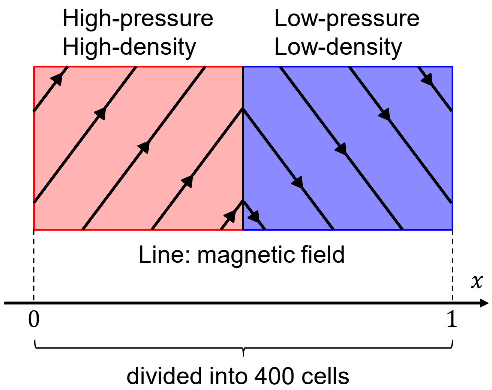

- The computational domain [0, 1] is divided into 400 uniform cells.
- The specific heat ratio is set to $\gamma = 2.0$.

[10] Brio, M., and Wu, C.C., “An upwind differencing scheme for the equations of ideal magnetohydrodynamics”, Journal of Computational Physics, vol. 75, 1988, pp.400–422.

Numerical example

■ MHD shock tube test [10]

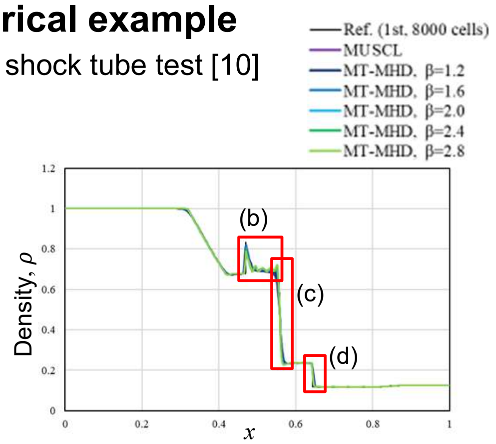

(a) Overall view

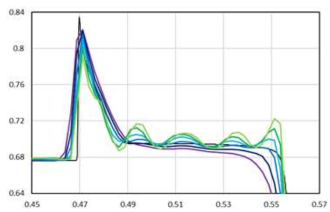

(b) Vicinity of compound wave

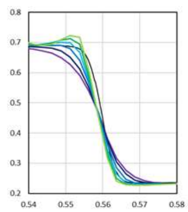

(c) Contact discontinuity

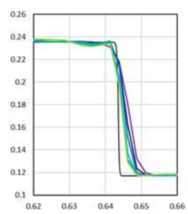

(d) Shock wave

Good: The MHD discontinuities are sharply captured by MT-MHD.
Bad : The solutions are oscillatory because of the complex phenomena of MHD (especially, the vicinity of the compound wave).
→ A more careful reconstruction strategy is necessary in MHD simulations

[10] Brio, M., and Wu, C.C., “An upwind differencing scheme for the equations of ideal magnetohydrodynamics”, Journal of Computational Physics, vol. 75, 1988, pp.400–422.

Outline

Analysis

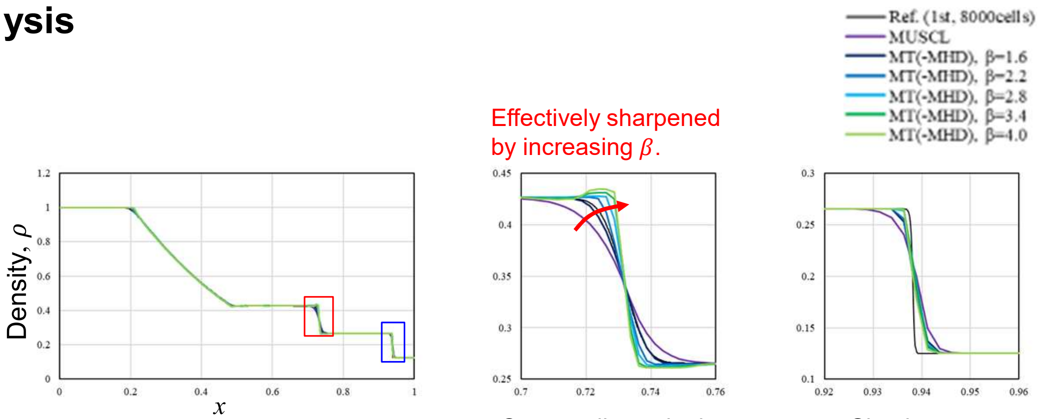

Contact discontinuity

Shock wave

- The contact discontinuity is effectively sharpened by increasing β.
- The sharpness of the shock tube is almost constant regardless of β.

→ Since nonlinear discontinuities, namely shock waves, have own mechanisms of physical compression, it is obvious that additional artificial compression is excessive.

Analysis

■ Time evolution of the density gradient

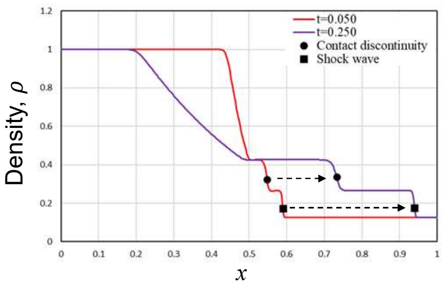

Density distributions of MUSCL

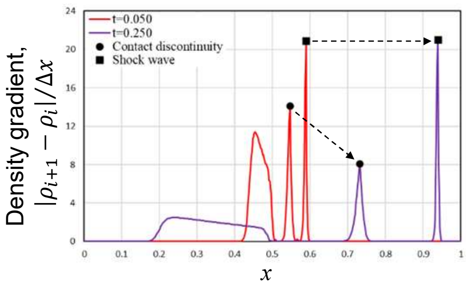

Density gradient distributions of MUSCL

The density gradient is defined as $g = |\rho_{i+1} - \rho_i|/\Delta x$.
We will observe the time evolution of the density gradient in the shock tube test of gas dynamics.

Analysis

■ Time evolution of the density gradient

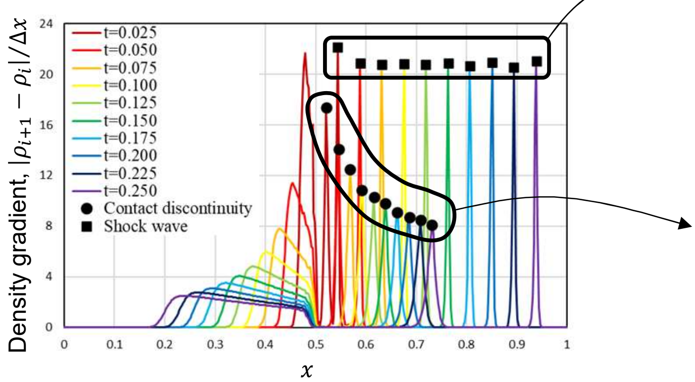

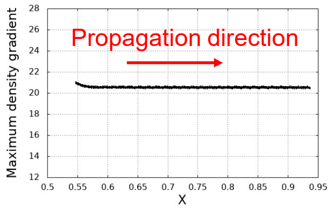

Trajectory of the shock wave from $t = 0.025$ to 0.25.

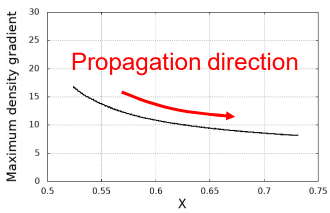

Trajectory of the contact discontinuity from $t = 0.025$ to 0.25.

Displaying the time evolution of the density gradient at shorter intervals,
we can see the trajectories of the sharpness of the contact discontinuity and shock wave.

Analysis

■ Trajectory: Effect of grid resolution

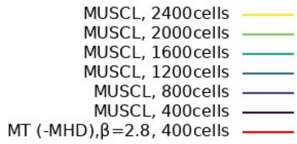

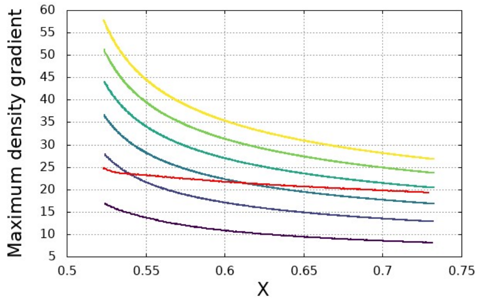

Contact discontinuity

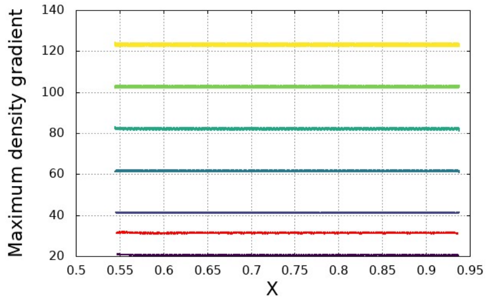

Shock wave

From these trajectory figures,
- the MUSCL calculations are significantly dissipative even using higher grid-resolution at the contact discontinuity.
  → MT-MHD becomes superior as the calculation time is longer because it can maintain the sharpness.
- the advantage of MT is not effective at the shock wave because the discontinuity does NOT dissipate even with MUSCL.

MT Targeting Linear discontinuity for MHD (MTTL-MHD)

■ Strategy of MTTL-MHD

From the above analyses,
- artificial compression to linear discontinuities can maintain its sharpness.
- artificial compression to nonlinear discontinuities is not so effective and may cause numerical oscillations due to excessive compression.

Strategy of the new scheme:
- Only the linear discontinuities are artificially compressed by THINC.
- The artificial compression of THINC is deactivated at nonlinear discontinuities.

Based on this strategy, we will replace the constant parameter β of MT-MHD by the following new β:

$$\beta = \phi\beta_{\max} + (1-\phi)\beta_{\min}$$

where ϕ is a weight function as

$$\phi \rightarrow \begin{cases} 0 & \text{for nonlinear regions} \\ 1 & \text{for linear regions} \end{cases}.$$

This modification allows linear discontinuities to be sharply captured and avoids excessive compression against nonlinear discontinuities.

MT Targeting Linear discontinuity for MHD (MTTL-MHD)

■ Weight function ϕ

Nonlinearity measure: Total pressure ratio $r_{pt} = \dfrac{p_{\mathrm{T,max}}}{p_{\mathrm{T,min}} + \varepsilon_z}$,

where total pressure is defined as

$$p_{\mathrm{T}} = p + \frac{|\boldsymbol{B}|^2}{2} = \text{gas pressure} + \text{magnetic pressure}.$$

The weight function ϕ is defined using this ratio as

$$\phi = \frac{1 - \cos(\pi\hat{\phi})}{2},$$

where

$$\hat{\phi} = \min\left\{1, \max\left(0, \frac{r_{pt,\max} - r_{pt}}{r_{pt,\max} - r_{pt,\min}}\right)\right\},$$

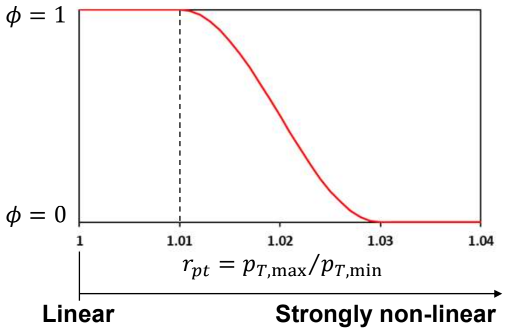

$$\beta = \phi\beta_{\max} + (1 - \phi)\beta_{\min}$$

$$\phi \to \begin{cases} 0 & \text{for nonlinear regions} \\ 1 & \text{for linear regions} \end{cases}$$

This ϕ behaves as shown in the right figure and can detect nonlinearity.
In this presentation, we will use $r_{pt,\max} = 1.03, r_{pt,\min} = 1.01, \beta_{\min} = 1.1.$

This new scheme will be called **MTTL-MHD** in this study.

Outline

Numerical example

■ MHD shock tube test [7]

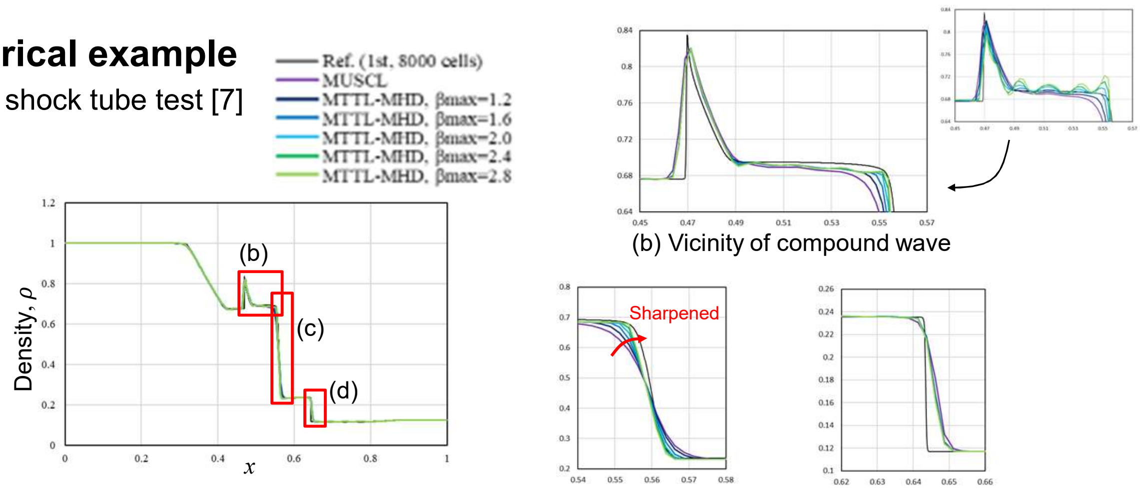

(a) Overall view (c) Contact discontinuity (d) Shock wave

- MTTL-MHD can calculate the vicinity of the compound wave without numerical oscillation.
- MTTL-MHD can effectively sharpen the contact discontinuity.

[7] Chiu, T. Y., Niu, Y. Y., and Chou, Y. J., "Accurate Hybrid AUSMD Type Flux Algorithm with Generalized Discontinuity Sharpening Reconstruction for Two-Fluid Modeling," J. Comput. Phys., 443 (2021), 110540.

Numerical example

■ MHD shock tube test [7]

MTTL-MHD with $\beta_{\text{max}} = 2.0, \beta_{\text{min}} = 1.1$

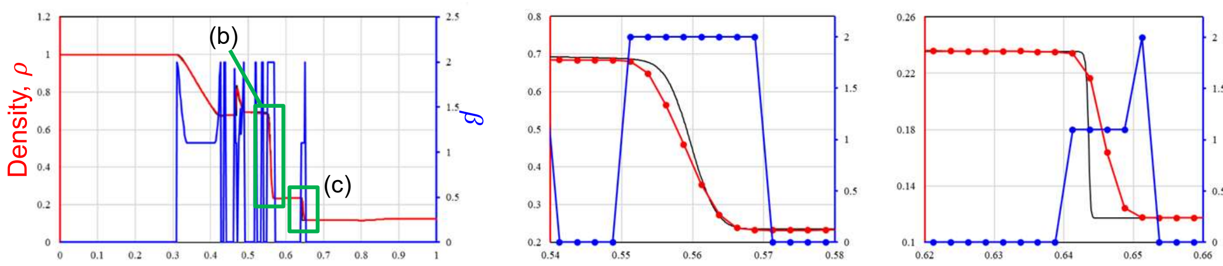

(a) Overall view (b) Contact discontinuity (c) Slow shock wave

- The large β is applied to the contact discontinuity.
- The small β is applied to the slow shock, and the artificial compression by THINC is deactivated.

→ MTTL-MHD can avoid excessive compression to nonlinear discontinuities and achieve robust and high resolution.

[7] Chiu, T. Y., Niu, Y. Y., and Chou, Y. J., "Accurate Hybrid AUSMD Type Flux Algorithm with Generalized Discontinuity Sharpening Reconstruction for Two-Fluid Modeling," J. Comput. Phys., 443 (2021), 110540.

Numerical example

■ MHD blast wave test (Gardiner & Stone, [11])

$$\begin{pmatrix} \rho \\ p \\ u \\ v \\ w \\ B_x \\ B_y \\ B_z \end{pmatrix}_{\mathrm{in}} = \begin{pmatrix} 1 \\ 10^2 \\ 0 \\ 0 \\ 0 \\ 10\sin\theta_0 \\ 10\cos\theta_0 \\ 0 \end{pmatrix}, \quad \begin{pmatrix} \rho \\ p \\ u \\ v \\ w \\ B_x \\ B_y \\ B_z \end{pmatrix}_{\mathrm{out}} = \begin{pmatrix} 1 \\ 1 \\ 0 \\ 0 \\ 0 \\ 10\sin\theta_0 \\ 10\cos\theta_0 \\ 0 \end{pmatrix}$$

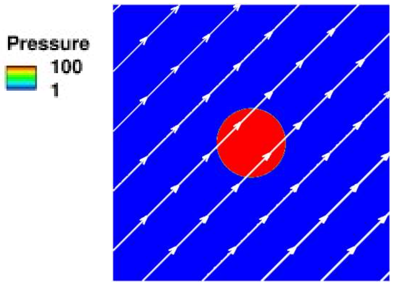

Line: initial magnetic field $\boldsymbol{B}$

- $\theta_0 = \pi/4$.
- Calculate the time evolution of the high-pressure region placed discontinuously in the center of the computational domain under the application of a magnetic field.
- The computational domain [-0.5, 0.5] × [-0.5, 0.5] is divided into 256 × 256 cells.
- The specific heat ratio is set to $\gamma = 5/3$.

[11] Gardiner, T.A., and Stone, J.M., "An unsplit Godunov method for ideal MHD via constrained transport", Journal of Computational Physics, vol. 205, 2005, pp.509–539.

Numerical example

■ MHD blast wave test (Gardiner & Stone, [11])

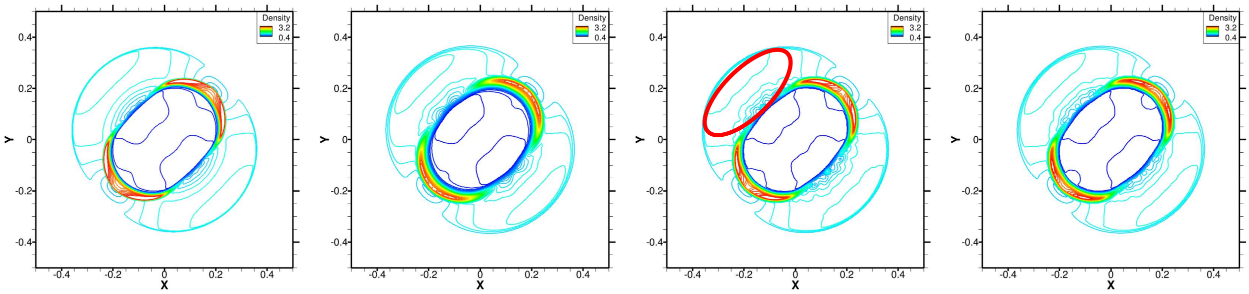

Reference (MUSCL, 1024x1024 cells) | MUSCL | MT-MHD ($\beta = 2.4$) | MTTL-MHD ($\beta_{\max} = 2.4$)

- Both MT-MHD and MTTL-MHD can solve this test without serious problem.
- MTTL-MHD can solve the regions surrounded by the red line more robustly than MT-MHD.

[11] Gardiner, T.A., and Stone, J.M., "An unsplit Godunov method for ideal MHD via constrained transport", Journal of Computational Physics, vol. 205, 2005, pp.509–539.

Numerical example

■ MHD blast wave test (Gardiner & Stone, [11])

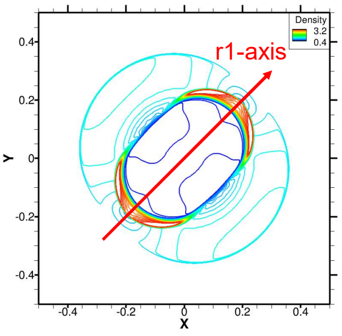

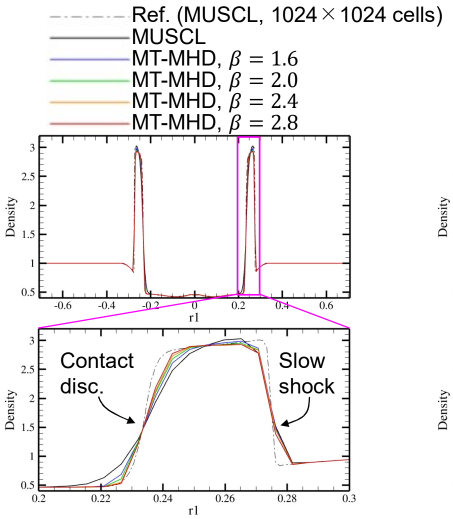

MT-MHD

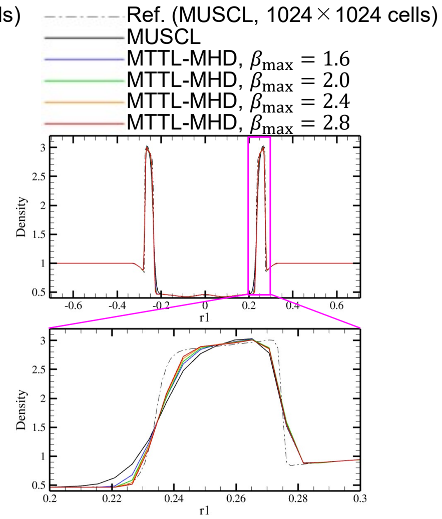

MTTL-MHD

Numerical example

■ MHD blast wave test (Gardiner & Stone, [11])

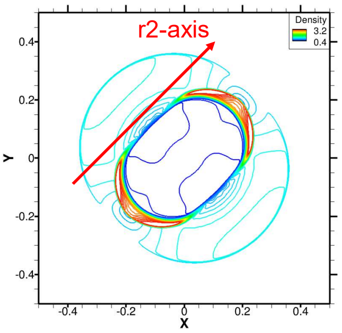

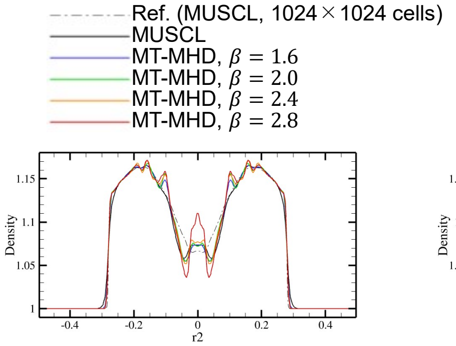

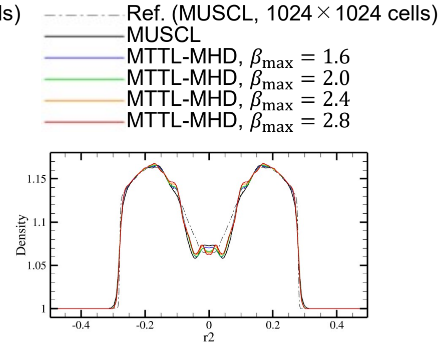

MTTL-MHD where the artificial compression is weakened at nonlinear discontinuities can solve this test more robustly than MT-MHD.

[11] Gardiner, T.A., and Stone, J.M., “An unsplit Godunov method for ideal MHD via constrained transport”, Journal of Computational Physics, vol. 205, 2005, pp.509–539.

Outline

Conclusion

In this study, we applied hybrid MUSCL-THINC to MHD simulations as MT-MHD and MTTL-MHD.
We obtained the following findings from the discussion using trajectories:

- Nonlinear discontinuities: Do not dissipate as time passes due to its own physical compression.
  Artificial compression to shock waves is excessive and results in numerical oscillations.

- Linear discontinuities: Do not have a mechanism to maintain sharpness and tend to dissipate as time passes.
  The artificial compression by THINC can maintain the sharpness effectively.

- By using physical information (in this study, nonlinearity) as well as the distribution shape of physical quantities, the performance of MT can be improved without increasing stencil size.

- The results of 1D and 2D MHD numerical tests showed that MTTL-MHD can sharply capture only linear discontinuities and avoid numerical oscillation due to excessive compression to nonlinear discontinuities.

Acknowledgments

We utilized CANS+ the open-source MHD numerical code "CANS+" (Coordinated Astronomical Numerical Software +, [12]) in this study. This work was supported by JSPS KAKENHI Grant Numbers JP23K26295, JP23KJ0981, JP23KJ0986.

We are grateful for the supports and the opportunity to use the tool.

[12] Matsumoto, Y., Asahina, Y., Kudoh, Y., Kawashima, T., Matsumoto, J., Takahashi, H. R., Minoshima, T., Zenitani, S., Miyoshi, T., and Matsumoto, R., "Magnetohydrodynamic simulation code CANS+: Assessments and applications", Publications of the Astronomical Society of Japan, vol. 00, No. 0, 2019, pp.1-26.

Supplement

Governing Equations

■ Ideal MHD equation (conservation form)

$$\frac{\partial \boldsymbol{U}}{\partial t} + \nabla \cdot \boldsymbol{F} = 0$$

$$\boldsymbol{U} = \begin{pmatrix} \rho \\ \rho\boldsymbol{v} \\ e \\ \boldsymbol{B} \end{pmatrix}, \boldsymbol{F} = \begin{pmatrix} \rho\boldsymbol{v} \\ \rho\boldsymbol{v}\boldsymbol{v} + p_T\boldsymbol{I} - \boldsymbol{B}\boldsymbol{B} \\ (e + p_T)\boldsymbol{v} - \boldsymbol{B}(\boldsymbol{v}\cdot\boldsymbol{B}) \\ \boldsymbol{v}\boldsymbol{B} - \boldsymbol{B}\boldsymbol{v} \end{pmatrix}$$

$$p_T = p + \frac{|\boldsymbol{B}|^2}{2}$$

$$e = \frac{p}{\gamma - 1} + \frac{\rho|\boldsymbol{u}|^2}{2} + \frac{|\boldsymbol{B}|^2}{2}$$

$\boldsymbol{U}$	: A vector of conservative variables
$\boldsymbol{F}$	: A flux vector
$\boldsymbol{I}$	: Identity matrix
ρ	: Density
$\boldsymbol{v} = (u \quad v \quad w)^T$	: A velocity vector
$\boldsymbol{B} = (B_x \quad B_y \quad B_z)^T$	: A magnetic field vector
p_T	: Total pressure
p	: Gas pressure
e	: Total energy density
γ	: Specific heat ratio

Governing Equations

■ 1D ideal MHD equation (discretization form)

$$\frac{\partial \boldsymbol{U}}{\partial t} + \nabla \cdot \boldsymbol{F} = 0, \qquad \boldsymbol{U} = \begin{pmatrix} \rho \\ \rho\boldsymbol{v} \\ e \\ \boldsymbol{B} \end{pmatrix}, \boldsymbol{F} = \begin{pmatrix} \rho\boldsymbol{v} \\ \rho\boldsymbol{v}\boldsymbol{v} + p_T\boldsymbol{I} - \boldsymbol{B}\boldsymbol{B} \\ (e + p_T)\boldsymbol{v} - \boldsymbol{B}(\boldsymbol{v}\cdot\boldsymbol{B}) \\ \boldsymbol{v}\boldsymbol{B} - \boldsymbol{B}\boldsymbol{v} \end{pmatrix}$$

$$\Big\downarrow \text{Discretization}$$

$$\boldsymbol{U}_i^{n+1} = \boldsymbol{U}_i^n - \frac{\delta t}{\Delta_i}\left(\widehat{\boldsymbol{F}}_{i+1/2} - \widehat{\boldsymbol{F}}_{i-1/2}\right)$$

δt	: A time step size
n	: A time step index
Δ_i	: A volume of a i-th cell
$\boldsymbol{U}_i^n$	: Physical quantities of a i-th cell at time $n\delta t$
$\widehat{\boldsymbol{F}}_{i\pm1}$	: Numerical fluxes at cell interfaces

Methodology

■ Behavior of ζ

$$\zeta = 1 - \min\left(\frac{\hat{V}^{\mathrm{MUSCL}}_{L,i+1/2} - \hat{V}^{\mathrm{MUSCL}}_{R,i-1/2} + \varepsilon_z}{V_{i+1} - V_i + \varepsilon_z}, \frac{\hat{V}^{\mathrm{MUSCL}}_{L,i+1/2} - \hat{V}^{\mathrm{MUSCL}}_{R,i-1/2} + \varepsilon_z}{V_i - V_{i-1} + \varepsilon_z}\right)$$

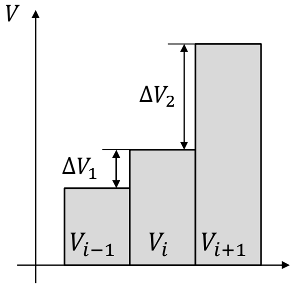

When the minmod limiter is used, …

$$\zeta = \frac{\max(\Delta V_1, \Delta V_2) - \min(\Delta V_1, \Delta V_2)}{\max(\Delta V_1, \Delta V_2)}$$

$\xleftrightarrow{\text{Compared}}$

A discretization form of a second derivative:

$$\frac{V_{i-1} - 2V_i + V_{i+1}}{\Delta x^2} = \frac{\max(\Delta V_1, \Delta V_2) - \min(\Delta V_1, \Delta V_2)}{\Delta x^2}$$

➡ ζ is equivalent to a distribution curvature normalized by $\max(\Delta V_1, \Delta V_2)$.

Numerical example

■ Shock tube test of gas dynamics [9]

$$q^{\mathrm{MT}} = (1 - \zeta) q^{\mathrm{MUSCL}} + \zeta q^{\mathrm{THINC}}$$

$$\zeta \to \begin{cases} 0 & \text{for continuous distributions} & \to \text{MUSCL is dominant.} \\ 1 & \text{for discontinuous distributions} & \to \text{THINC is dominant.} \end{cases}$$

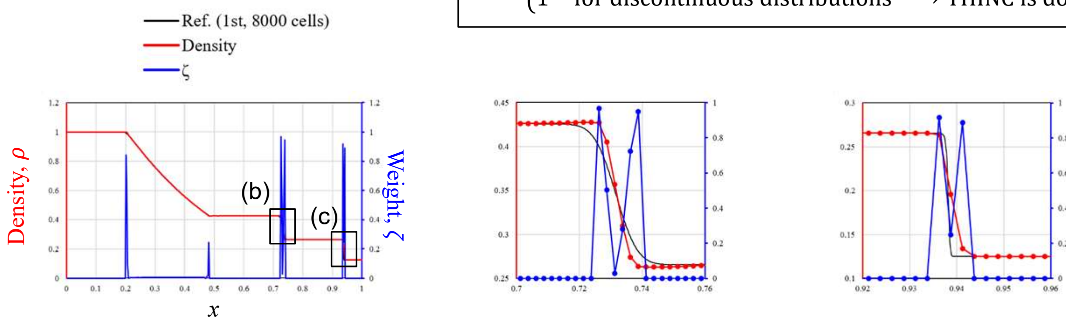

(a) Overall view (b) Contact discontinuity (c) Shock wave

ζ works as a curvature detector and has a large value at the heads and tails of the discontinuities.

[9] Sod, G. A., "A Survey of Several Finite Difference Methods for Systems of Nonlinear Hyperbolic Conservation Laws", Journal of Computational Physics, vol. 27, No. 1, 1978, pp.1–31.

Methodology

■ Monotonicity confirmation in MT-MHD

When a target cell is located at a local extremum, the cell is not reconstructed (namely, 1st-order accuracy) because the hyperbolic tangent function cannot be defined. Therefore, it is necessary to confirm either the stencil has a monotone or extremum profile. For this confirmation, we use a following inequality:

$$(V_{i+1} - V_i)(V_i - V_{i-1}) > \varepsilon_M,$$

where ε_M is a tolerance value, and we used $\varepsilon_M = 10^{-6}$. This inequality can avoid unnecessary computation of THINC when monotone distributions accidentally occur owing to small numerical errors. This enables reduction of calculation costs and improvement of robustness in practical calculations.

Analysis

■ Trajectory: Effect of β

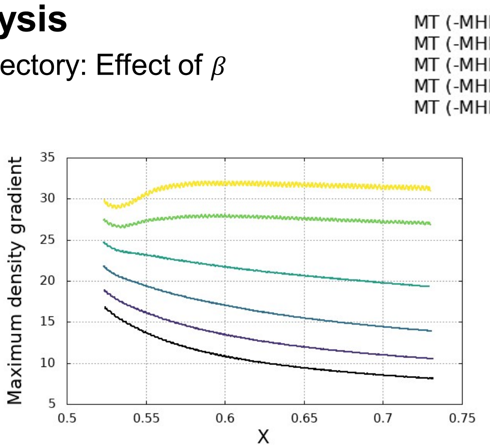

Contact discontinuity

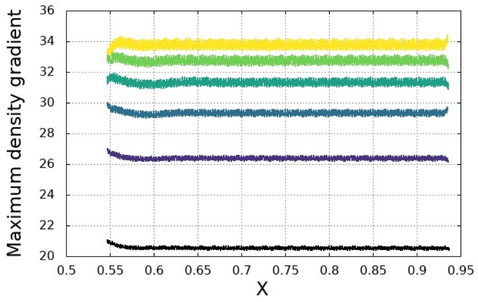

Shock wave

From these trajectory figures,

- the larger β can maintain the sharpness of the contact discontinuity as the calculation time passes.
- the sharpness of the shock wave does NOT dissipate as the time passes even if only MUSCL is used.

Analysis

■ Trajectory smoothing process (1/2)

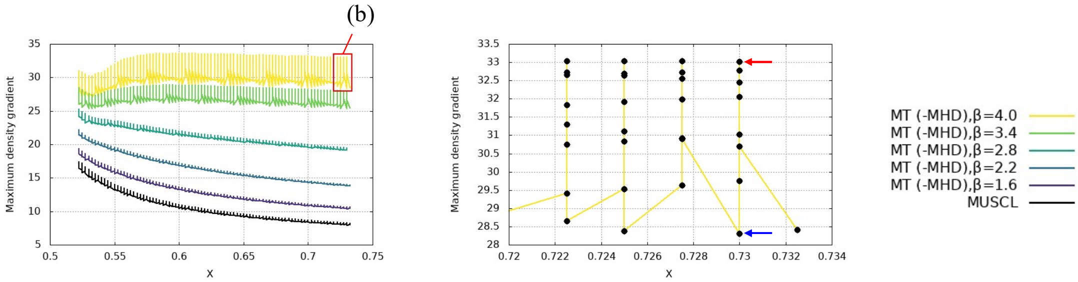

(a) The unsmoothed trajectories of the shock tube test of gas dynamics

The trajectories used in above slides were smoothed by moving average for ease of viewing. This is because unsmoothed trajectories are oscillatory as shown in Fig. (a). Figure (b) shows the density distributions in the vicinity of the discontinuity at the maximum and minimum extrema of the trajectory as shown in Fig. (a). From this figure, the reason of the oscillations of the trajectories is that the cell that has the maximum density gradient is identical for several time steps. Since these oscillations are not relevant to the discussion, we smoothed the trajectories using moving average for ease of viewing and avoiding confusion.

Analysis

■ Trajectory smoothing process (2/2)

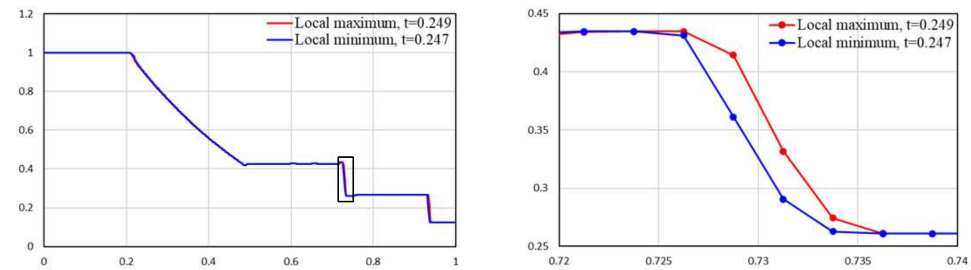

(b) The density distributions of the shock tube test of gas dynamics which correspond the local minimum and maximum shown in Fig. (a).

The trajectories used in above slides were smoothed by moving average for ease of viewing. This is because unsmoothed trajectories are oscillatory as shown in Fig. (a). Figure (b) shows the density distributions in the vicinity of the discontinuity at the maximum and minimum extrema of the trajectory as shown in Fig. (a). From this figure, the reason of the oscillations of the trajectories is that the cell that has the maximum density gradient is identical for several time steps. Since these oscillations are not relevant to the discussion, we smoothed the trajectories using moving average for ease of viewing and avoiding confusion.